Human induced pluripotent stem cell-derived cardiomyocytes to study inflammation-induced aberrant calcium transient

Yuki Tatekoshi[1,#], Chunlei Chen[1,#], Jason Shapiro[1], Hsiang-Chun Chang[1], Malorie Blancard[2], Davi Lyra-Leite[2], Paul W. Burridge[2], Matthew Feinstein[3], Richard D'Aquila[3], Priscilla Hsue[4], and Hossein Ardehali[1,2,3]

[1]Feinberg Cardiovascular and Renal Research Institute, and [2]Department of Pharmacology, [3]Department of Medicine, Northwestern University, Chicago, IL
[4]Department of Medicine, University of California at San Francisco, San Francisco, CA

[#]These authors contributed equally.

Address correspondence to:
Hossein Ardehali
SQBRC 8-521
303 E Superior Street
Chicago, Illinois 60611, USA.
Phone: 312.503.2342
Email: h-ardehali@northwestern.edu

Abstract
Heart failure with preserved ejection fraction (HFpEF) is commonly found in persons living with HIV (PLWH) even when antiretroviral therapy (ART) suppresses HIV viremia. However, studying this condition has been challenging because an appropriate animal model is not available. In this paper, we studied calcium transient in human induced pluripotent stem cell-derived cardiomyocytes (hiPSC-CMs) in culture to simulate the cardiomyocyte relaxation defect noted in of PLWH and HFpEF and to assess whether various drugs have an effect. We show that treatment of hiPSC-CMs with inflammatory cytokines (such as interferon-γ or TNF-α) impair their Ca^{2+} uptake into sarcoplasmic reticulum and that SGLT2 inhibitors, clinically proven as effective for HFpEF, reverse this effect. Additionally, treatment with mitochondrial antioxidants (like mito-Tempo) and certain antiretrovirals resulted in the reversal of the effects of these cytokines on calcium transient. Finally, incubation of hiPSC-CMs with serum from HIV patients with and without diastolic dysfunction did not alter their Ca^{2+}-decay time, indicating that the exposure to the serum of these patients is not sufficient to induce the decrease in Ca^{2+} uptake *in vitro*. Together, our results indicate that hiPSC-CMs can be used as a model to study molecular mechanisms of inflammation-mediated abnormal cardiomyocyte relaxation and screen for potential new interventions.

Introduction

Heart failure (HF) with preserved ejection fraction (HFpEF) refers to a form of HF that is associated with diastolic dysfunction (DD). On echocardiography, HFpEF is associated with a greater than 50% of blood in the left ventricle (LV) is pumped with each beat but the LV displays impaired relaxation and increased stiffness during the filling phase of cardiac cycle. Echocardiographic evidence of DD is associated with higher all-cause mortality even in asymptomatic patients (1). The pathophysiology underlying DD is known to be an increase in the stiffness of the LV, although there are limited ways to study mechanisms and interventions. Studies have shown that patients with HFpEF have multiple comorbidities, such as obesity, hypertension, renal dysfunction, and diabetes (2,3) and that it is associated with aging (4). It is also proposed that these comorbid conditions each lead to increased systemic inflammation which then causes myocardial remodeling and fibrosis (2,5-7).

There are few options for the treatment of HFpEF, despite the increasing incidence of this disease in HIV-uninfected and -infected patients. The current treatments relieve symptoms and target comorbid conditions, such as hypertension, diabetes, coronary artery disease, hyperlipidemia, and atrial fibrillation. Although beta blockers (BB), ACE inhibitors (ACEI), angiotensin receptor blockers (ARB), and cardiac resynchronization therapy improve outcome in patients with HF with reduced ejection fraction (HFrEF), clinical benefits have scarcely been shown with any of these drugs in HFpEF. The only drugs that have shown clinical benefit in rigorous trials are antagonists of the mineralocorticoid receptor (MRA, such as spironolactone) (8), inhibitors of the sodium glucose co-transporter 2 (SGLT2, such as empagliflozin) (9), and glucagon-like peptide 1 analogue (GLP-1, such as semaglutide) (10).

Persons living with HIV (PLWH) have a higher prevalence of HFpEF compared to uninfected individuals (11,12). Recent studies have shown that LV mass index and DD are each significantly worse in PLWH with HFpEF than among persons living without HIV with HFpEF, despite similar EF. These features were associated with lower nadir $CD4^+$ T-cell count, suggesting that this process could be due to the level of immunodeficiency and/or duration of untreated infection (13). Several studies attempted to determine the mechanism for increased HFpEF in PLWH. Administration of HIV gp120 resulted in DD after adrenergic stimulation in rats (14), and caused negative inotropic effects in adult rat ventricular myocytes (15,16). Macaques infected with simian immunodeficiency virus (SIV) display DD, which was associated with the degree of myocardial SIV viral load. Inhibition of CCR5, a co-receptor with CD4 for HIV gp120-mediated entry into cells, in the SIV-infected rhesus macaque model of DD preserved cardiac diastolic function (17).

Untreated HIV infection is associated with circulating inflammatory cytokines and chemokines (18), and many remain elevated even when HIV viremia is well-controlled by antiretroviral therapy (ART) (19,20). For instance, elevated IFN-γ is observed during acute HIV viremia and remained elevated despite highly active ART (HAART) (21). Higher IFN-γ is also associated with impaired CD4 recovery in HIV after the initiation of HAART (22). Additionally, while the immune system resets itself after the regression of bacterial or viral infection, it remains hypersensitive when ART suppresses viremia in chronic HIV infection. Of note, monocytes from PLWH treated with viremia suppressing ART demonstrated increased production of TNF-α and IL-6 after stimulation with lipopolysaccharide (23), indicating the presence of immune system rewiring during HIV infection that is not reversed with effective ART. Therefore, cardiomyocytes in PLWH are exposed to higher circulating inflammatory cytokines at baseline despite effective ART, and with further elevation of these inflammatory cytokines after concomitant infections. Among these cytokines, TNF-α is associated with mortality (24) and severe coronary stenosis (greater than 70% stenosis) (25) in PLWH.

There are limited studies to address the molecular basis of cardiomyocyte dysfunction in HIV-mediated HFpEF or the effectiveness of various drugs. Additionally, there are currently no models using

human heart cells and HIV. These major limitations raise the critical need for a novel approach to study this complicated disease. Human induced pluripotent stem cell (hiPSC)-derived cardiomyocytes (hiPSC-CM) represent a novel technology that has been successfully applied to understanding basic mechanisms of several cardiovascular diseases, including long QT (26), LEOPARD (27) and Timothy (28) syndromes, dilated cardiomyopathy (CM) (29,30) and hypertrophic CM (30). They are also used for efficacy and toxicity screening of drugs (31,32), leading to enhanced understanding of cellular mechanisms at the single cardiomyocyte level, not previously possible using human cells. Furthermore, hiPSC-CMs have been used to study a model of viral myocarditis (i.e., coxsackie virus) and to predict the efficacy of antiviral drug therapies (33), indicating that these cells can be used to study HF due to viral infections. In this paper, we show that hiPSC-CMs can be used as a model for the assessment of calcium transient in response to inflammatory cytokines *in vitro* and to assess the effects of various drugs on their relaxation parameters. Given the major limitations in the field of HIV-mediated cardiac dysfunction, this model will allow investigators to study the mechanism of cardiac DD in inflammatory condition *in vitro* and assess the effectiveness of various drugs to reverse impaired relaxation noted with systemic inflammation.

Results

TNF-α and IFN-γ impair relaxation in hiPSC-CMs without causing cellular damage

We first generated hiPSCs and differentiated into cardiomyocytes using the protocols previously published by our groups (34). Successful production of hiPSC-CMs were confirmed by the assessment of their morphology and calcium transient property (**Figure 1-figure supplement 1A and B, and -video supplement 1**). We then assessed whether treatment with cytokines would have detrimental effects on these cells. Because DD has been associated with mitochondrial dysfunction (35), we first measure whether cytokine treatment results in changes of mitochondrial membrane potential (MMP) at baseline. For these experiments, cells were treated with cytokines at indicated concentrations for 48 hours. These studies revealed that each of the cytokines studied in our system did not alter MMP in hiPSC-CMs (**Figure 1-figure supplement 1C**). For the remaining studies, we focused our experiments on two of these cytokines that often are chronically increased in PLWH, TNF-α and IFN-γ.

We next assessed whether treatment with TNF-α or IFN-γ alters diastolic function in hiPSC-CMs by measuring calcium transient and assessing the decay time and downstroke time in these cells using Single Cell Kinetic Image Cytometry (Vala science). Treatment with both TNF-α and IFN-γ resulted in a significant increase in decay time and downstroke time, which are markers of cardiomyocyte relaxation, while beats per minute (indirect measurement of heart rate and not diastolic function) was essentially unchanged (**Figure 1A-C**). Additionally, treatment with mitoTempo (an agent with mitochondrial antioxidant activity) reversed the changes that occurred with TNF-α (**Figure 1A and B**), indicating that a reduction in mitochondrial reactive oxygen species (ROS) may, at least partially, reverse the cardiomyocyte relaxation defect induced by TNF-α.

Since mitoTempo partially reversed the effects of TNF-α on calcium transient of hiPSC-CMs, we next assessed whether TNF-α and IFN-γ have any effects on mitochondrial respiration and whether these potential defects would be reversed with antioxidants. For these experiments, we used Seahorse XF96 Analyzer to measure the oxygen consumption rate (OCR) after treatment with TNF-α or IFN-γ in the presence and absence of the general antioxidant, N-acetylcysteine (NAC). While both TNF-α and IFN-γ did not induce significant changes in OCR, administration of NAC to hiPSC-CMs supplemented with TNF-α significantly reduced OCR at baseline (**Figure 2**). These data indicate that the beneficial effects of antioxidant reagents on calcium transient might be associated with the alleviation of aberrantly regulated OCR in TNF-α-treated cells. We next used this platform to study the effects of various drugs on *in vitro* measures of DD.

Certain antiviral drugs and SGLT2 inhibitors reverse impaired relaxation in hiPSC-CMs

Given that we were able to induce impaired relaxation indicated by aberrant Ca^{2+} uptake in hiPSC-CMs after treatment with inflammatory cytokines, we assessed whether various antiretrovirals and other drugs that potentially target the pathogenesis of HFpEF can reverse the dysregulation of calcium transient *in vitro*. We first assessed whether ART drugs at various concentrations cause cell death or increased ROS production in hiPSC-CMs. We treated hiPSC-CMs with tenofovir (a nucleotide-analog reverse transcriptase inhibitor), darunavir (a protease inhibitor), raltegravir and elvitegravir (integrase inhibitors) at concentrations between 3 μM – 10 mM. The dose range was chosen to extend to 10-fold above the IC50 concentrations and reflects the upper range of circulating drug concentration in patients receiving these medications (36-39). In this dose range, we did not observe apparent changes in cell viability and cellular ROS levels (**Figure 3-figure supplement 1A and B**), indicating that exposure to these single drugs alone has minimal effects on cell survival.

We then assessed whether ART can reverse the impaired relaxation induced by TNF-α. For these studies, we used the following single drug concentrations: 5 μM tenofovir, 10 μM darunavir, 3 μM raltegravir, and 10 μM emtricitabine (an HIV nucleoside analog reverse transcriptase inhibitor). As

shown in **Figure 3**, while TNF-α increased the decay time in hiPSC-CMs, treatment with tenofovir, darunavir, raltegravir, and emtricitabine reversed these effects. These results indicate that ART may have beneficial effects on the inflammation-mediated deterioration of calcium transient that occurs in HIV patients, raising the possibility that its potential benefits may go beyond their inhibitory effects on the virus itself.

A number of other drugs have also been proposed to potentially exert beneficial effects in HFpEF. Among these, we focused on an oral soluble guanylate cyclase (sGC) stimulator (riociguat,1 μM), a phosphodiesterase (PDE)-5 inhibitor (sildenafil, 1μM), a PDE9 inhibitors (PF-04447943, 5 μM) and a SGLT2 inhibitor (dapagliflozin, 10 μM). The dosages are based on previous functional studies in isolated cardiomyocytes (40-44). Specifically, we also tested 1 μM of dapagliflozin and found no effects on decay and downstroke times (**Figure 4-figure supplement 1A and B**). While TNF-α caused a significant increase in decay time in hiPSC-CMs, riociguat, sildenafil and PF-04447943 failed to reverse this effect (**Figure 4A-C**), indicating that they do not have the properties to reverse the inflammation-mediated impaired relaxation. However, SGLT2 inhibitor dapagliflozin significantly reversed the prolonged decay and downstroke times induced by TNF-α in hiPSC-CMs (**Figure 4D-G**). Additionally, we repeated the experiments with IFN-γ and dapagliflozin and showed that the drug was able to reverse the increased decay and downstroke time associated with IFN-γ as well (**Figure 4H-K**). These studies are in accordance with the clinical studies that have shown beneficial effects of SGLT2 inhibitors in HFpEF and suggest that they may also benefit patients with inflammation-induced aberrant calcium transient, like HIV+ patients.

Treatment with serum from patients with HIV does not induce impaired relaxation in hiPSC-CMs

Given that we could simulate impaired calcium transient in hiPSC-CMs using inflammatory cytokines, we next assessed whether short-term treatment of these cells with serum from HIV+ patients with evidence of DD would also induce impaired Ca^{2+} uptake in the cells. We used two sources of serum in our studies. For the first group, we recruited six men with chronic HIV on ART with undetectable viral loads who underwent cardiac magnetic resonance imaging (CMRI) at the Northwestern Memorial Hospital (NMH) for assessment of myocardial perfusion reserve (MPR). Clinical and MRI-based characteristics of these patients are included in **Supplementary Table 1**. Lower values of myocardial perfusion reserve (MPR) indicate impaired global myocardial blood flow in response to vasodilator stress and are associated with higher incidence of HFpEF and poor prognosis (45,46). The second group included well-controlled patients with HIV at University of California San Francisco (UCSF) with echocardiographic evidence of normal cardiac function or DD.

For both groups, we treated hiPSC-CMs with 10% serum from these patients for 48 hours, followed by measurement of calcium transients. Additionally, we treated human umbilical vein endothelial cells (HUVEC) with the serum of these patients for 20 hours and assessed their angiogenic potential given the critical relationship between endothelial dysfunction and the development of HFpEF (47,48). For the first group of patients, we stratify into higher (1.9-3.4; N=3) versus lower (1.0-1.1; N=3) MPR values, which correspond to control and DD, respectively. As shown in **Figure 5A-C**, serum from HIV+ patients with DD from group 1 did not result in a significant change in decay and downstroke time in hiPSC-CMs. Similar results were obtained after 24-hour incubation. Additionally, serum from these patients did not alter the tube network formation of HUVECs (**Figure 5D-G** and **Figure 5-figure supplement 1 and 2**). We also assessed the effects of serum from HIV+ patients from group 2. The control group for experiments included serum from HIV patients without evidence of DD. Our data indicate that treatment of hiPSC-CMs and HUVECs with 2% serum of these patients for 3 or 24 hours does not alter decay time (**Figure 6A-D)** and tube formation capacity (**Figure 6E-I**), respectively. For hiPSC-CMs studies, we exposed the cells to serum for 3 hours and 24 hours and did not observe a difference in decay time with either time point. These results suggest that short-treatment of hiPSC-CMs or HUVECs with serum

from patients with DD does not induce changes in calcium transient or their angiogenic potential, respectively.

Discussion

HFpEF is a common disease and its incidence continues to increase. Among risk factors for HFpEF, inflammation is believed to be a common mechanism for the development of the disease. The chronic inflammatory condition associated with treated HIV infection is believed to be responsible for the development of HFpEF in these patients. Despite the high incidence of this disorder among the general population and those with HIV, there are currently very few systems available to study this disorder and to screen for drugs that can target the disease. In this paper, we used hiPSC-CMs as a platform to assess whether abnormal cardiomyocyte relaxation can be induced in these cells in response to inflammatory cytokines. We demonstrate that TNF-α and IFN-γ can induce prolonged decay time in hiPSC-CMs, which can partially be reversed with mitochondrially targeted antioxidants. We also demonstrate that most ART drugs and SGLT2 inhibitors can reverse the aberrant calcium transient associated with inflammatory cytokines. Finally, to determine whether treatment of hiPSC-CMs serum from patients with HIV and DD can also induce deterioration of calcium transient in hiPSC-CMs, we treated these cells with patient serum, but were not able to mimic DD. We also assessed whether serum from these patients can induce defects in angiogenic potential and found no effects on these parameters. Overall, our results provide a novel platform to study dysregulated calcium transient associated with inflammatory cytokine treatment and to test the effectiveness of various agents in this disorder.

Studying HFpEF in tissue culture has its own limitations, since HFpEF is a systemic disorder and usually develops as a result of a number of risk factors, including diabetes, hypertension and chronic kidney disease. It is important to note that DD is a major component of HFpEF and studying the relaxation abnormalities associated with this disorder, especially in tissue culture setting, can provide major clues to this disease at the cellular level. Thus, using a cell culture system to mimic the functional abnormality noted in this disorder can provide clues to the disease that can later be tested at the organismal level. Given that there are limited animal models for HFpEF, an *in vitro* model will provide a powerful platform for hypothesis generation and drug screening prior to committing resources for studying these findings at the organismal level.

We demonstrated that treatment with certain cytokines can induce prolonged decay time in hiPSC-CMs, but serum from HIV patients with imaging evidence of DD did not cause similar abnormalities. This could be due to several reasons, including short duration of the treatment with human serum, lower concentration of cytokines in the serum compared to the concentration we used in our studies, and possibly differences in gene expression patterns between human matured cardiomyocytes and hiPSC-CMs. In fact, previous studies demonstrated lower concentrations of TNF-α and IFN-γ (41.32 pg/ml and 0.78 pg/ml, respectively) in HIV+ patient serum than ones adopted in this study (49,50). Because of the limited availability of serum samples from HIV patients, we were not able to test different concentration and duration of serum treatment in our hiPSC-CM system. Further experiments with serum from HIV+ with DD in a large-scale are warranted to determine whether other conditions can induce aberrant calcium transient. Nevertheless, it is important to note that cytokines alone can induce impaired Ca^{2+} uptake in hiPSC-CMs and can be used to induce this condition *in vitro*.

It is surprising that SGLT2 inhibitors reversed the progression of DD in our system, since cardiomyocytes do not express SGLT2 under physiological conditions. Interestingly, Marfella et al. reported that adult cardiomyocytes express SGLT2 in diabetic conditions (51). Since diabetes is associated with low grade systemic inflammation, HIV patients might also express SGLT2 in their cardiomyocytes. Taken together, our data indicate that SGLT2 inhibitors at the

dosages used in this study reverse the impaired calcium transients induced by TNF-α and IFN-γ. Additionally, the fact that ART drugs were able to reverse the impaired Ca^{2+} uptake associated with cytokine treatment raise the possibility that these drugs can prevent damage to cardiomyocyte function as a result of the inflammation associated with HIV, in addition to their anti-retroviral effects.

There are limitations with our studies. Although decay and downstroke time were utilized as surrogates of cardiomyocyte relaxation, direct biomechanical characterization of contraction was not conducted in our study. While cytosolic calcium concentration is a major factor in the regulation of cellular relaxation (52), certain conditions, including the transition of sarcomere protein isoforms to pathogenic ones (53) and stimulation of β-adrenergic receptors (54) can alter this relationship. However, since hiPSC-CMs utilized for each study is from iPS cells derived from a single donor, we believe that these parameters had minimal effects in our system. We also did not elucidate the molecular mechanisms underlying prolonged decay time induced by TNF-α and IFN-γ. TNF-α treatment is reported to induce a longer decay of calcium transient and a decreased sarcoplasmic ATPase (SERCA) expression in rabbit cardiomyocytes from pulmonary vein (55) Thus, our observation in hiPSC-CMs may also be through decreased expression of SERCA though further studies remain conducted. Darunavir is generally used in combination with ritonavir and elvitegravir along with cobicistat in clinical practice. These additional drugs were not tested in our studies. Additionally, our studies employed only single drugs, which is not commonly used in the clinic. Also. we did not perform a dose-response curve with the drugs we tested, but used concentrations that were reported previously. Another limitation of our study is that we did not determine the mechanism of how ART drugs with such different effects on HIV proteins can have an effect on cellular relaxation. This is an important issue, and further studies are needed to better assess the mechanism of how ART can exert such effects.

In summary, we provide a novel approach to study inflammation-induced calcium transient at the cellular level using hiPSC-CMs. We use this method to test a number of drugs and whether they can reverse the prolonged decay time associated with inflammation. This system can prove useful in studying the molecular basis and potential treatments for HFpEF induced by chronic inflammation.

Figure legends

Figure 1. Normalized downstroke time (**A**), decay time (**B**), and beating rate as assessed by beats per minute (**C**) in hiPSC-CM treated with bovine serum albumin (BSA), (control), TNF-α, IFN-γ, TNF-α plus mitoTempo, and IFN-γ plus mitoTempo. N=5-14**.** Data were analyzed by ordinary one-way ANOVA and post-hoc Tukey's multiple comparison test. Bars represent group mean.

Figure 2. OCR in hiPSC-CM treated with cytokines and antioxidant agent NAC. **(A)** OCR trace of hiPSC-CM treated with BSA, TNF-α, IFN-γ, TNF-α+IFN-γ, TNF-α+NAC, IFN-γ+NAC, and TNF-α+IFN-γ+NAC. (**B-D**) Bar graph summary of data in Panel A with OCR at baseline (**B**), after adding carbonyl cyanide m-chlorophenyl hydrazone (CCCP) (**C**), and after adding antimycin A and rotenone (**D**). N=5-6. Data were analyzed by ordinary one-way ANOVA and post-hoc Tukey's multiple comparison test. Bars represent group mean.

Figure 3. Decay time in hiPSC-CM after treatment with TNF-α and various ART drugs. (**A**) Decay time after treatment with TNF-α, tenofovir, and TNF-α+tenofovir. (**B**) Decay time after treatment with TNF-α, darunavir, and TNF-α+darunavir. (**C**) Decay time after treatment with TNF-α, raltegravier, and TNF-α+ raltegravier. (**D**) Decay time after treatment with TNF-α, emtricitabine, and TNF-α+ emtricitabine. N=5-21. Data were analyzed by ordinary one-way ANOVA and post-hoc Tukey's multiple comparison test. Bars represent group mean.

Figure 4. Decay time in hiPSC-CM after treatment with TNF-α and riociguat, sildenafil citrate, PF-04447943, and dapagliflozin. (**A**) Decay time after treatment with TNF-α, sGS agonist riociguat, and TNF-α+riociguat. (**B**) Decay time after treatment with TNF-α, sildenafil citrate, and TNF-α+sildenafil citrate. (**C**) Decay time after treatment with TNF-α, PF-04447943, and TNF-α+PF-04447943. (**D**) Representative curve of calcium transient in hiPSC-CM treated with TNF-α, dapagliflozin, and TNF-α+dapagliflozin. (**E**) Curve of derivative calculated with data in panel **(D)**. (**F**) Decay time after treatment with TNF-α, dapagliflozin, and TNF-α+dapagliflozin. (**G**) Downstroke time after treatment with TNF-α, dapagliflozin, and TNF-α+dapagliflozin. (**H**) Representative curve of calcium transient in hiPSC-CM treated with IFN-γ, dapagliflozin, and IFN-γ+dapagliflozin. (**I**) Curve of derivative calculated with data in panel **(H)**. (**J**) Decay time after treatment with INF-γ, dapagliflozin, and IFN-γ+dapagliflozin. (**K**) Downstroke time after treatment with INF-γ, dapagliflozin, and IFN-γ+dapagliflozin. (N=5-21. Data were analyzed by ordinary one-way ANOVA and post-hoc Tukey's multiple comparison test. Bars represent group mean.

Figure 5. Ca^{2+}-decay time of hiPSC-CM and angiogenic function of ECs after treatment with serum from Group 1 HIV+ patients with DD. (**A-C**) Pooled normalized decay time (**A**), downstroke time (**B**) and beating rate (**C**) in hiPSC treated with 10% serum for 48 hours from group 1 HIV+ patients with DD. (**D-G**) Angiogenic parameters, including total length of branching (**D**), (N = 3), number of junctions (**E**) (N = 3), total length (**F**) (N =3) and number of meshes (**G**) (N = 3) in HUVECs after treatment with 2% serum from Group 1 patients for 20 hours. Data were analyzed by unpaired Student's *t* test. Bars represent group mean.

Figure 6. Diastolic function of hiPSC-CMs and angiogenic function of ECs after treatment with serum from HIV+ patients with DD (Group 2). (**A-B**) Individual normalized decay time 3 hours (N=3-9) (**A**) or 24 hours (N=3-13) (**B**) after treatment of hiPSC-CM with 2% serum from patients. (**C-D**) Pooled decay time data from patients in panels A and B with 3 hour (**C**) and 24 hours (**D**) after treatment with serum. (**E**) Representative image of formed tube structure with cultured HUVECs treated with serum from HIV+ patients with DD. (**F-I**) Assessment of tube formation of

HUVECs 20 hours after treatment with serum of patients, including number of meshes (**F**) (N = 8), number of junctions (**G**) (N = 8), number of segments (**H**) (N = 8) and total length of branching (**I**) (N = 8). Data were analyzed by unpaired Student's *t* test for (**C, D, F, G, H and I**). Bars represent group mean.

Supplemental Figure Legends

Figure 1-figure supplement 1. (**A**) Representative image of hiPSC-CM. Scale bar represents 100 μm. (**B**) Representative curves of calcium transient and its derivative in hiPSC-CM. (**C**) MMP as assessed by tetramethylrhodamine ethyl ester (TMRE) in hiPSC-CM treated with various cytokines. Concentration of cytokines used is as follows: CCL3 1nM, TNF-α 300 pg/ml, IL-6 1 ng/ml, IL-1β 200 pg/ml, IP-10 (or CXCL10) 500 pg/ml, IFN-γ 1ng/ml. N=4, Data were analyzed by ordinary one-way ANOVA and post-hoc Tukey's multiple comparison test. Bars represent group mean.

Figure 3-figure supplement 1. Cell viability (**A**) and cellular ROS levels (**B**) in hiPSC-CM exposed to concentrations ranging from between 3nM and 10μM of tenofovir (a nucleotide-analog reverse transcriptase inhibitor), darunavir (a protease inhibitor), raltegravir and elvitegravir (integrase inhibitors).

Figure 4-figure supplement 1. Decay time (**A**) and downstroke time (**B**) in hiPSC-CM after treatment with TNF-α and 1 μM of dapagliflozin. N = 5-21, Data were analyzed by ordinary one-way ANOVA and post-hoc Tukey's multiple comparison test. Bars represent group mean.

Figure 5-figure supplement 1. Representative images of formed tube structure with HUVECs treated with 2% serum from HIV+ patients with high or low MPR for 20 hours.

Figure 5-figure supplement 2. Representative magnified images of formed tube structure with HUVECs treated with 2% serum from HIV+ patients with high or low MPR for 20 hours.

Supplemental Video Legends

Figure 1-video supplement 1. Representative video of hiPSC-CMs contracting spontaneously in a culture dish.

Methods

Human Induced Pluripotent Cell Derivation and Cardiac differentiation

Protocols and consents were approved by the institutional review board of Northwestern University. The hiPSC from healthy individuals was generated following the protocol published before (56). The hiPSC were maintained and differentiated into beating cardiomyocytes, according to the previously published protocol (34).

MMP measurement

Media was removed from hiPSC-CM and were washed with phosphate-buffered saline (PBS) and FluoroBrite DMEM (No Glutamine, No HEPES, No Phenol Red, No Sodium Pyruvate, Thermo A1896702) was added. Cells were stained with 5 nM TMRE (for mitochondrial stain) for 20 min and then washed with PBS before immunofluorescence. TMRE (red channel) signal was analyzed as MMP using ImageJ (FIJI).

Seahorse assay

7 days before assay, hiPSC-CMs were plated at 100,000 cells per well in Matrigel coated Seahorse XF cell culture 96-well plate. The day before the assay, the Seahorse cartridge was placed in the XF calibrant and incubated overnight at 37 ºC. On the day of the assay, the plates were incubated at RT for 1 hr in glucose free complete DMEM or RPMI without bicarbonate or phenol-red to allow even distribution of cells across the well floor. Before placing the sample plates in the Seahorse XF96 Analyzer, media volume was adjusted to 150 µl in each well. 25 mM glucose, 1.5 mM Oligomycin, 1 µM CCCP, and 20 µM rotenone (Rot)/ antimycin A (AA), were diluted in DMEM and injected sequentially into each well, following the standard Seahorse protocol. Cytokine treatment was started 48 hours before Seahorse assay.

Treatment of hiPSC with IFN-γ and TNF-α

hiPSC-CMs after 21-24 days culturing were seeded into 6 wells or 96 wells cell culture plates. After 5 days, IFN-γ at 1 ng/ml and TNF-α at 300 pg/ml were added to the cells for 48 hrs.

Drug concentrations

We used the following drug concentrations for our studies: riociguat - 1 µM, sildenafil citrate - 1 µM, PF-04447943 - 5 µM, dapagliflozin - 1 or 10 µM, tenofovir - 5 µM, emtricitabine - 10 µM, darunavir - 10 µM, raltegravir - 3 µM.

Calcium transient studies in hiPSC-CM

For Ca^{2+} transient analysis, Day 21-24 hiPSC-CMs were plated on the Matrigel coated 96 well black cell culture plate, at a density of 75,000 cells/well. Calcium imaging was performed as described previously (57). On the day of imaging (Day 28-32), cells were stained with a buffer containing 5 µM Fluo-4AM, NucBlue (2 drops/10ml), 2.5 mM probenecid, 0.02% Pluronic F-127 in FluoroBrite DMEM for 1 hr at 37 °C, 5% CO_2. After 1h incubation, aspirate dye loading solution and add 200 µl FluoroBrite DMEM to each well for imaging. Single Cell Kinetic Image Cytometry (vala science) was used to scan the plate and CyteSeer Automated Video Analysis Software (vala science) was used to analyze the Ca^{2+} transient.

Tube formation assay

The formation of tube networks was assessed as described before (58). HUVECs (Lonza) were seeded at 20,000 per well in a 96-well plate coated with 75 mL Matrigel (Fisher Scientific) or Cultrex (R & D Systems) reduced growth factor basement membrane matrix. The cells were treated with EBM-2 medium containing 2% serum from HIV+ patients obtained from NMH and UCSF wherever mentioned. Following a 20 hour-incubation, tube networks from each biological replicate were analyzed in at least

three random fields by light microscopy. The number of branch points (junctions), segments and meshes, and total length of tubule networks (total length of branching) were quantified by Fiji software (Angiogenesis Analyzer).

Participant samples

Blood samples from 6 men with chronic HIV on ART with undetectable viral loads who underwent CMRI for assessment of MPR were used. For CMRI, all scanning was performed on 1.5T MRI scanners (Siemens Medical Systems), with participants receiving FDA-approved intravenous double-dosing of gadolinium contrast followed by adenosine as the vasodilator agent. Images were performed at maximal hyperemia (vasodilation) and compared with rest: MPR was calculated as the ratio of stress myocardial blood flow to rest myocardial blood flow as described previously (59). Comparisons in hiPSC-CM performance characteristics were made between those with higher (1.9-3.4; N=3) versus lower (1.0-1.1; N=3) MPR values; additional clinical and MRI-based characteristics are included in **Supplementary Table 1**. The study was approved by the Institutional Review Board of Northwestern University (STU00204874).

Serum samples from UCSF are from an IRB-approved (IRB# 10-03112) longitudinal cohort study evaluating the pathogenesis of HIV and HHV-8 to pulmonary hypertension. PLWH underwent serial phlebotomy, transthoracic echocardiogram, flow-mediated dilation, 6-minute walk test and pulse wave velocity measurements. Subset of participants underwent a right heart catheterization. The study is IRB-approved, and participants provided signed informed consent prior to undergoing study procedures. Serum samples are derived from documented HIV-positive individuals on stable ART and have diastolic function assessed by echocardiogram. Samples are de-identified and stored long term with UCSF's AIDS Specimen Bank (ASB).

Of the 16 participants included from UCSF, median age was 54.1 (IQR 45.0, 57.1), median duration of HIV infection was 17 years (IQR 12.7, 22.7), median CD4 count was 395 (IQR 334, 645), 88% were male, 50% were Caucasian, 37% were African American, and 13% were Hispanic/Latino. Comorbidities included 43.8% had hypertension, 31.3% had hyperlipidemia, 12.5% had diabetes, and 62.5% were current or past smokers. All specimens were matched case-control to those with DD to those without DD.

Baseline echocardiogram characteristics included everyone with preserved LV systolic function (≥50%). In the DD group, n=2 had grade 1 DD, n=3 had grade 2 DD, and n=3 had grade 3 DD. Two individuals in DD group had mild left atrial enlargement (LA volume index 35-41 mL/m^2). Five individuals in the DD group and two in the control group had RVSP ≥35mmHg.

12 participants (6 from each group) underwent right heart catheterization with two in the DD group had elevated mean pulmonary arterial pressure (mPAP) (≥25 mmHg). Three participants in the DD group and two in the control group had right atrial pressure >5 mmHg.

Statistical analysis

Data are presented as mean ± SEM. Unpaired Student t-test and one-way ANOVA, with post hoc Tukey's test were conducted to assess statistical significant difference among experimental groups. A P-value less than 0.05 was considered statistically significant.

References

1. Kardys, I., Deckers, J. W., Stricker, B. H., Vletter, W. B., Hofman, A., and Witteman, J. C. (2009) Echocardiographic parameters and all-cause mortality: the Rotterdam Study. *International journal of cardiology* **133**, 198-204
2. Dhingra, A., Garg, A., Kaur, S., Chopra, S., Batra, J. S., Pandey, A., Chaanine, A. H., and Agarwal, S. K. (2014) Epidemiology of heart failure with preserved ejection fraction. *Current heart failure reports* **11**, 354-365
3. Haass, M., Kitzman, D. W., Anand, I. S., Miller, A., Zile, M. R., Massie, B. M., and Carson, P. E. (2011) Body mass index and adverse cardiovascular outcomes in heart failure patients with preserved ejection fraction: results from the Irbesartan in Heart Failure with Preserved Ejection Fraction (I-PRESERVE) trial. *Circulation. Heart failure* **4**, 324-331
4. Xu, B., and Daimon, M. (2016) Cardiac aging phenomenon and its clinical features by echocardiography. *Journal of echocardiography* **14**, 139-145
5. Cheng, J. M., Akkerhuis, K. M., Battes, L. C., van Vark, L. C., Hillege, H. L., Paulus, W. J., Boersma, E., and Kardys, I. (2013) Biomarkers of heart failure with normal ejection fraction: a systematic review. *European journal of heart failure* **15**, 1350-1362
6. Sanders-van Wijk, S., van Empel, V., Davarzani, N., Maeder, M. T., Handschin, R., Pfisterer, M. E., Brunner-La Rocca, H. P., and investigators, T.-C. (2015) Circulating biomarkers of distinct pathophysiological pathways in heart failure with preserved vs. reduced left ventricular ejection fraction. *European journal of heart failure* **17**, 1006-1014
7. Santhanakrishnan, R., Chong, J. P., Ng, T. P., Ling, L. H., Sim, D., Leong, K. T., Yeo, P. S., Ong, H. Y., Jaufeerally, F., Wong, R., Chai, P., Low, A. F., Richards, A. M., and Lam, C. S. (2012) Growth differentiation factor 15, ST2, high-sensitivity troponin T, and N-terminal pro brain natriuretic peptide in heart failure with preserved vs. reduced ejection fraction. *European journal of heart failure* **14**, 1338-1347
8. Pfeffer, M. A., and Braunwald, E. (2016) Treatment of Heart Failure With Preserved Ejection Fraction: Reflections on Its Treatment With an Aldosterone Antagonist. *JAMA cardiology* **1**, 7-8
9. Anker, S. D., Butler, J., Filippatos, G., Ferreira, J. P., Bocchi, E., Bohm, M., Brunner-La Rocca, H. P., Choi, D. J., Chopra, V., Chuquiure-Valenzuela, E., Giannetti, N., Gomez-Mesa, J. E., Janssens, S., Januzzi, J. L., Gonzalez-Juanatey, J. R., Merkely, B., Nicholls, S. J., Perrone, S. V., Pina, I. L., Ponikowski, P., Senni, M., Sim, D., Spinar, J., Squire, I., Taddei, S., Tsutsui, H., Verma, S., Vinereanu, D., Zhang, J., Carson, P., Lam, C. S. P., Marx, N., Zeller, C., Sattar, N., Jamal, W., Schnaidt, S., Schnee, J. M., Brueckmann, M., Pocock, S. J., Zannad, F., Packer, M., and Investigators, E. M.-P. T. (2021) Empagliflozin in Heart Failure with a Preserved Ejection Fraction. *N Engl J Med* **385**, 1451-1461
10. Kosiborod, M. N., Abildstrom, S. Z., Borlaug, B. A., Butler, J., Rasmussen, S., Davies, M., Hovingh, G. K., Kitzman, D. W., Lindegaard, M. L., Moller, D. V., Shah, S. J., Treppendahl, M. B., Verma, S., Abhayaratna, W., Ahmed, F. Z., Chopra, V., Ezekowitz, J., Fu, M., Ito, H., Lelonek, M., Melenovsky, V., Merkely, B., Nunez, J., Perna, E., Schou, M., Senni, M., Sharma, K., Van der Meer, P., von Lewinski, D., Wolf, D., Petrie, M. C., Committees, S. T.-H. T., and Investigators. (2023) Semaglutide in Patients with Heart Failure with Preserved Ejection Fraction and Obesity. *N Engl J Med* **389**, 1069-1084
11. Meng, Q., Lima, J. A., Lai, H., Vlahov, D., Celentano, D. D., Strathdee, S., Nelson, K. E., Tong, W., and Lai, S. (2002) Use of HIV protease inhibitors is associated with left ventricular morphologic changes and diastolic dysfunction. *J Acquir Immune Defic Syndr* **30**, 306-310

12. Schuster, I., Thoni, G. J., Ederhy, S., Walther, G., Nottin, S., Vinet, A., Boccara, F., Khireddine, M., Girard, P. M., Mauboussin, J. M., Rouanet, I., Dauzat, M., Cohen, A., Messner-Pellenc, P., and Obert, P. (2008) Subclinical cardiac abnormalities in human immunodeficiency virus-infected men receiving antiretroviral therapy. *The American journal of cardiology* **101**, 1213-1217
13. Hsue, P. Y., Hunt, P. W., Ho, J. E., Farah, H. H., Schnell, A., Hoh, R., Martin, J. N., Deeks, S. G., and Bolger, A. F. (2010) Impact of HIV infection on diastolic function and left ventricular mass. *Circulation. Heart failure* **3**, 132-139
14. Berzingi, C., Chen, F., and Finkel, M. S. (2009) p38 MAP kinase inhibitor prevents diastolic dysfunction in rats following HIV gp120 injection in vivo. *Cardiovascular toxicology* **9**, 142-150
15. Kan, H., Xie, Z., and Finkel, M. S. (2004) p38 MAP kinase-mediated negative inotropic effect of HIV gp120 on cardiac myocytes. *American journal of physiology. Cell physiology* **286**, C1-7
16. Yuan, Y., Kan, H., Fang, Q., Chen, F., and Finkel, M. S. (2008) CXCR4 receptor antagonist blocks cardiac myocyte p38 MAP kinase phosphorylation by HIV gp120. *Cardiovascular toxicology* **8**, 173-180
17. Kelly, K. M., Tocchetti, C. G., Lyashkov, A., Tarwater, P. M., Bedja, D., Graham, D. R., Beck, S. E., Metcalf Pate, K. A., Queen, S. E., Adams, R. J., Paolocci, N., and Mankowski, J. L. (2014) CCR5 inhibition prevents cardiac dysfunction in the SIV/macaque model of HIV. *Journal of the American Heart Association* **3**, e000874
18. Katsikis, P. D., Mueller, Y. M., and Villinger, F. (2011) The cytokine network of acute HIV infection: a promising target for vaccines and therapy to reduce viral set-point? *PLoS pathogens* **7**, e1002055
19. Keating, S. M., Golub, E. T., Nowicki, M., Young, M., Anastos, K., Crystal, H., Cohen, M. H., Zhang, J., Greenblatt, R. M., Desai, S., Wu, S., Landay, A. L., Gange, S. J., Norris, P. J., and Women's Interagency, H. I. V. S. (2011) The effect of HIV infection and HAART on inflammatory biomarkers in a population-based cohort of women. *Aids* **25**, 1823-1832
20. Ramirez, L. A., Arango, T. A., Thompson, E., Naji, M., Tebas, P., and Boyer, J. D. (2014) High IP-10 levels decrease T cell function in HIV-1-infected individuals on ART. *J Leukoc Biol* **96**, 1055-1063
21. Roff, S. R., Noon-Song, E. N., and Yamamoto, J. K. (2014) The Significance of Interferon-gamma in HIV-1 Pathogenesis, Therapy, and Prophylaxis. *Front Immunol* **4**, 498
22. Watanabe, D., Uehira, T., Suzuki, S., Matsumoto, E., Ueji, T., Hirota, K., Minami, R., Takahama, S., Hayashi, K., Sawamura, M., Yamamoto, M., and Shirasaka, T. (2019) Clinical characteristics of HIV-1-infected patients with high levels of plasma interferon-gamma: a multicenter observational study. *BMC Infect Dis* **19**, 11
23. Amirayan-Chevillard, N., Tissot-Dupont, H., Capo, C., Brunet, C., Dignat-George, F., Obadia, Y., Gallais, H., and Mege, J. L. (2000) Impact of highly active anti-retroviral therapy (HAART) on cytokine production and monocyte subsets in HIV-infected patients. *Clinical and experimental immunology* **120**, 107-112
24. Wada, N. I., Bream, J. H., Martinez-Maza, O., Macatangay, B., Galvin, S. R., Margolick, J. B., and Jacobson, L. P. (2016) Inflammatory Biomarkers and Mortality Risk Among HIV-Suppressed Men: A Multisite Prospective Cohort Study. *Clin Infect Dis* **63**, 984-990
25. Bahrami, H., Budoff, M., Haberlen, S. A., Rezaeian, P., Ketlogetswe, K., Tracy, R., Palella, F., Witt, M. D., McConnell, M. V., Kingsley, L., and Post, W. S. (2016) Inflammatory Markers Associated With Subclinical Coronary Artery Disease: The Multicenter AIDS Cohort Study. *Journal of the American Heart Association* **5**

26. Itzhaki, I., Maizels, L., Huber, I., Zwi-Dantsis, L., Caspi, O., Winterstern, A., Feldman, O., Gepstein, A., Arbel, G., Hammerman, H., Boulos, M., and Gepstein, L. (2011) Modelling the long QT syndrome with induced pluripotent stem cells. *Nature* **471**, 225-229
27. Carvajal-Vergara, X., Sevilla, A., D'Souza, S. L., Ang, Y. S., Schaniel, C., Lee, D. F., Yang, L., Kaplan, A. D., Adler, E. D., Rozov, R., Ge, Y., Cohen, N., Edelmann, L. J., Chang, B., Waghray, A., Su, J., Pardo, S., Lichtenbelt, K. D., Tartaglia, M., Gelb, B. D., and Lemischka, I. R. (2010) Patient-specific induced pluripotent stem-cell-derived models of LEOPARD syndrome. *Nature* **465**, 808-812
28. Yazawa, M., Hsueh, B., Jia, X., Pasca, A. M., Bernstein, J. A., Hallmayer, J., and Dolmetsch, R. E. (2011) Using induced pluripotent stem cells to investigate cardiac phenotypes in Timothy syndrome. *Nature* **471**, 230-234
29. Sun, N., Yazawa, M., Liu, J., Han, L., Sanchez-Freire, V., Abilez, O. J., Navarrete, E. G., Hu, S., Wang, L., Lee, A., Pavlovic, A., Lin, S., Chen, R., Hajjar, R. J., Snyder, M. P., Dolmetsch, R. E., Butte, M. J., Ashley, E. A., Longaker, M. T., Robbins, R. C., and Wu, J. C. (2012) Patient-specific induced pluripotent stem cells as a model for familial dilated cardiomyopathy. *Sci. Transl. Med.* **4**, 130ra147
30. Lan, F., Lee, A. S., Liang, P., Sanchez-Freire, V., Nguyen, P. K., Wang, L., Han, L., Yen, M., Wang, Y., Sun, N., Abilez, O. J., Hu, S., Ebert, A. D., Navarrete, E. G., Simmons, C. S., Wheeler, M., Pruitt, B., Lewis, R., Yamaguchi, Y., Ashley, E. A., Bers, D. M., Robbins, R. C., Longaker, M. T., and Wu, J. C. (2013) Abnormal calcium handling properties underlie familial hypertrophic cardiomyopathy pathology in patient-specific induced pluripotent stem cells. *Cell Stem Cell* **12**, 101-113
31. Liang, P., Lan, F., Lee, A. S., Gong, T., Sanchez-Freire, V., Wang, Y., Diecke, S., Sallam, K., Knowles, J. W., Wang, P. J., Nguyen, P. K., Bers, D. M., Robbins, R. C., and Wu, J. C. (2013) Drug screening using a library of human induced pluripotent stem cell-derived cardiomyocytes reveals disease-specific patterns of cardiotoxicity. *Circulation* **127**, 1677-1691
32. Navarrete, E. G., Liang, P., Lan, F., Sanchez-Freire, V., Simmons, C., Gong, T., Sharma, A., Burridge, P. W., Patlolla, B., Lee, A. S., Wu, H., Beygui, R. E., Wu, S. M., Robbins, R. C., Bers, D. M., and Wu, J. C. (2013) Screening drug-induced arrhythmia [corrected] using human induced pluripotent stem cell-derived cardiomyocytes and low-impedance microelectrode arrays. *Circulation* **128**, S3-13
33. Sharma, A., Marceau, C., Hamaguchi, R., Burridge, P. W., Rajarajan, K., Churko, J. M., Wu, H., Sallam, K. I., Matsa, E., Sturzu, A. C., Che, Y., Ebert, A., Diecke, S., Liang, P., Red-Horse, K., Carette, J. E., Wu, S. M., and Wu, J. C. (2014) Human induced pluripotent stem cell-derived cardiomyocytes as an in vitro model for coxsackievirus B3-induced myocarditis and antiviral drug screening platform. *Circ Res* **115**, 556-566
34. Burridge, P. W., Holmstrom, A., and Wu, J. C. (2015) Chemically Defined Culture and Cardiomyocyte Differentiation of Human Pluripotent Stem Cells. *Curr Protoc Hum Genet* **87**, 21 23 21-21 23 15
35. Kumar, A. A., Kelly, D. P., and Chirinos, J. A. (2019) Mitochondrial Dysfunction in Heart Failure With Preserved Ejection Fraction. *Circulation* **139**, 1435-1450
36. Droste, J. A., Verweij-van Wissen, C. P., Kearney, B. P., Buffels, R., Vanhorssen, P. J., Hekster, Y. A., and Burger, D. M. (2005) Pharmacokinetic study of tenofovir disoproxil fumarate combined with rifampin in healthy volunteers. *Antimicrobial agents and chemotherapy* **49**, 680-684
37. Kakuda, T. N., Brochot, A., Tomaka, F. L., Vangeneugden, T., Van De Casteele, T., and Hoetelmans, R. M. (2014) Pharmacokinetics and pharmacodynamics of boosted once-daily darunavir. *The Journal of antimicrobial chemotherapy* **69**, 2591-2605
38. Shiomi, M., Matsuki, S., Ikeda, A., Ishikawa, T., Nishino, N., Kimura, M., Kumagai, Y., and Irie, S. (2015) Pharmacokinetic and bioequivalence evaluation of single-tablet and

separate-tablet regimens for once-daily cobicistat-boosted elvitegravir in healthy Japanese male subjects: A randomized, two-way crossover study. *Clinical pharmacology in drug development* **4**, 218-225
39. Wang, L., Soon, G. H., Seng, K. Y., Li, J., Lee, E., Yong, E. L., Goh, B. C., Flexner, C., and Lee, L. (2011) Pharmacokinetic modeling of plasma and intracellular concentrations of raltegravir in healthy volunteers. *Antimicrobial agents and chemotherapy* **55**, 4090-4095
40. Castro, L. R., Verde, I., Cooper, D. M., and Fischmeister, R. (2006) Cyclic guanosine monophosphate compartmentation in rat cardiac myocytes. *Circulation* **113**, 2221-2228
41. Kiso, H., Ohba, T., Iino, K., Sato, K., Terata, Y., Murakami, M., Ono, K., Watanabe, H., and Ito, H. (2013) Sildenafil prevents the up-regulation of transient receptor potential canonical channels in the development of cardiomyocyte hypertrophy. *Biochemical and biophysical research communications* **436**, 514-518
42. Lee, D. I., Zhu, G., Sasaki, T., Cho, G. S., Hamdani, N., Holewinski, R., Jo, S. H., Danner, T., Zhang, M., Rainer, P. P., Bedja, D., Kirk, J. A., Ranek, M. J., Dostmann, W. R., Kwon, C., Margulies, K. B., Van Eyk, J. E., Paulus, W. J., Takimoto, E., and Kass, D. A. (2015) Phosphodiesterase 9A controls nitric-oxide-independent cGMP and hypertrophic heart disease. *Nature* **519**, 472-476
43. Reinke, Y., Gross, S., Eckerle, L. G., Hertrich, I., Busch, M., Busch, R., Riad, A., Rauch, B. H., Stasch, J. P., Dorr, M., and Felix, S. B. (2015) The soluble guanylate cyclase stimulator riociguat and the soluble guanylate cyclase activator cinaciguat exert no direct effects on contractility and relaxation of cardiac myocytes from normal rats. *European journal of pharmacology* **767**, 1-9
44. Zhang, S., Rodriguez, R., Scholz, P. M., and Weiss, H. R. (2006) Functional interaction of a beta-adrenergic agonist and cyclic GMP phosphodiesterase inhibitor in control and hypertrophic cardiomyocytes. *Pharmacology* **76**, 53-60
45. Arnold, J. R., Kanagala, P., Budgeon, C. A., Jerosch-Herold, M., Gulsin, G. S., Singh, A., Khan, J. N., Chan, D. C. S., Squire, I. B., Ng, L. L., and McCann, G. P. (2022) Prevalence and Prognostic Significance of Microvascular Dysfunction in Heart Failure With Preserved Ejection Fraction. *JACC Cardiovasc Imaging* **15**, 1001-1011
46. Markley, R., Del Buono, M. G., Mihalick, V., Pandelidis, A., Trankle, C., Jordan, J. H., Decamp, K., Winston, C., Carbone, S., Billingsley, H., Barron, A., Thomas, G., Van Tassell, B., Hundley, W. G., Kellman, P., and Abbate, A. (2023) Abnormal left ventricular subendocardial perfusion and diastolic function in women with obesity and heart failure and preserved ejection fraction. *Int J Cardiovasc Imaging* **39**, 811-819
47. Cornuault, L., Rouault, P., Duplaa, C., Couffinhal, T., and Renault, M. A. (2022) Endothelial Dysfunction in Heart Failure With Preserved Ejection Fraction: What are the Experimental Proofs? *Front Physiol* **13**, 906272
48. Paulus, W. J., and Tschope, C. (2013) A novel paradigm for heart failure with preserved ejection fraction: comorbidities drive myocardial dysfunction and remodeling through coronary microvascular endothelial inflammation. *J Am Coll Cardiol* **62**, 263-271
49. Musa, F., Shaviya, N., Mambo, F., Abonyo, C., Barasa, E., Wafula, P., Sowayi, G., Barasa, M., and Were, T. (2021) Cytokine profiles in highly active antiretroviral treatment non-adherent, adherent and naive HIV-1 infected patients in Western Kenya. *Afr Health Sci* **21**, 1584-1592
50. Osuji, F. N., Onyenekwe, C. C., Ahaneku, J. E., and Ukibe, N. R. (2018) The effects of highly active antiretroviral therapy on the serum levels of pro-inflammatory and anti-inflammatory cytokines in HIV infected subjects. *J Biomed Sci* **25**, 88
51. Marfella, R., Scisciola, L., D'Onofrio, N., Maiello, C., Trotta, M. C., Sardu, C., Panarese, I., Ferraraccio, F., Capuano, A., Barbieri, M., Balestrieri, M. L., Napoli, C., and Paolisso,

G. (2022) Sodium-glucose cotransporter-2 (SGLT2) expression in diabetic and non-diabetic failing human cardiomyocytes. *Pharmacol Res* **184**, 106448
52. Feridooni, H. A., Dibb, K. M., and Howlett, S. E. (2015) How cardiomyocyte excitation, calcium release and contraction become altered with age. *Journal of molecular and cellular cardiology* **83**, 62-72
53. Fentzke, R. C., Buck, S. H., Patel, J. R., Lin, H., Wolska, B. M., Stojanovic, M. O., Martin, A. F., Solaro, R. J., Moss, R. L., and Leiden, J. M. (1999) Impaired cardiomyocyte relaxation and diastolic function in transgenic mice expressing slow skeletal troponin I in the heart. *J Physiol* **517 (Pt 1)**, 143-157
54. Bers, D. M., Xiang, Y. K., and Zaccolo, M. (2019) Whole-Cell cAMP and PKA Activity are Epiphenomena, Nanodomain Signaling Matters. *Physiology (Bethesda)* **34**, 240-249
55. Lee, S. H., Chen, Y. C., Chen, Y. J., Chang, S. L., Tai, C. T., Wongcharoen, W., Yeh, H. I., Lin, C. I., and Chen, S. A. (2007) Tumor necrosis factor-alpha alters calcium handling and increases arrhythmogenesis of pulmonary vein cardiomyocytes. *Life Sci* **80**, 1806-1815
56. Churko, J. M., Burridge, P. W., and Wu, J. C. (2013) Generation of human iPSCs from human peripheral blood mononuclear cells using non-integrative Sendai virus in chemically defined conditions. *Methods in molecular biology* **1036**, 81-88
57. Romero-Tejeda, M., Fonoudi, H., Weddle, C. J., DeKeyser, J. M., Lenny, B., Fetterman, K. A., Magdy, T., Sapkota, Y., Epting, C. L., and Burridge, P. W. (2023) A novel transcription factor combination for direct reprogramming to a spontaneously contracting human cardiomyocyte-like state. *Journal of molecular and cellular cardiology* **182**, 30-43
58. Das, A., Huang, G. X., Bonkowski, M. S., Longchamp, A., Li, C., Schultz, M. B., Kim, L. J., Osborne, B., Joshi, S., Lu, Y., Trevino-Villarreal, J. H., Kang, M. J., Hung, T. T., Lee, B., Williams, E. O., Igarashi, M., Mitchell, J. R., Wu, L. E., Turner, N., Arany, Z., Guarente, L., and Sinclair, D. A. (2018) Impairment of an Endothelial NAD(+)-H(2)S Signaling Network Is a Reversible Cause of Vascular Aging. *Cell* **173**, 74-89 e20
59. Lee, D. C., and Johnson, N. P. (2009) Quantification of absolute myocardial blood flow by magnetic resonance perfusion imaging. *JACC Cardiovasc Imaging* **2**, 761-770

Figure 1

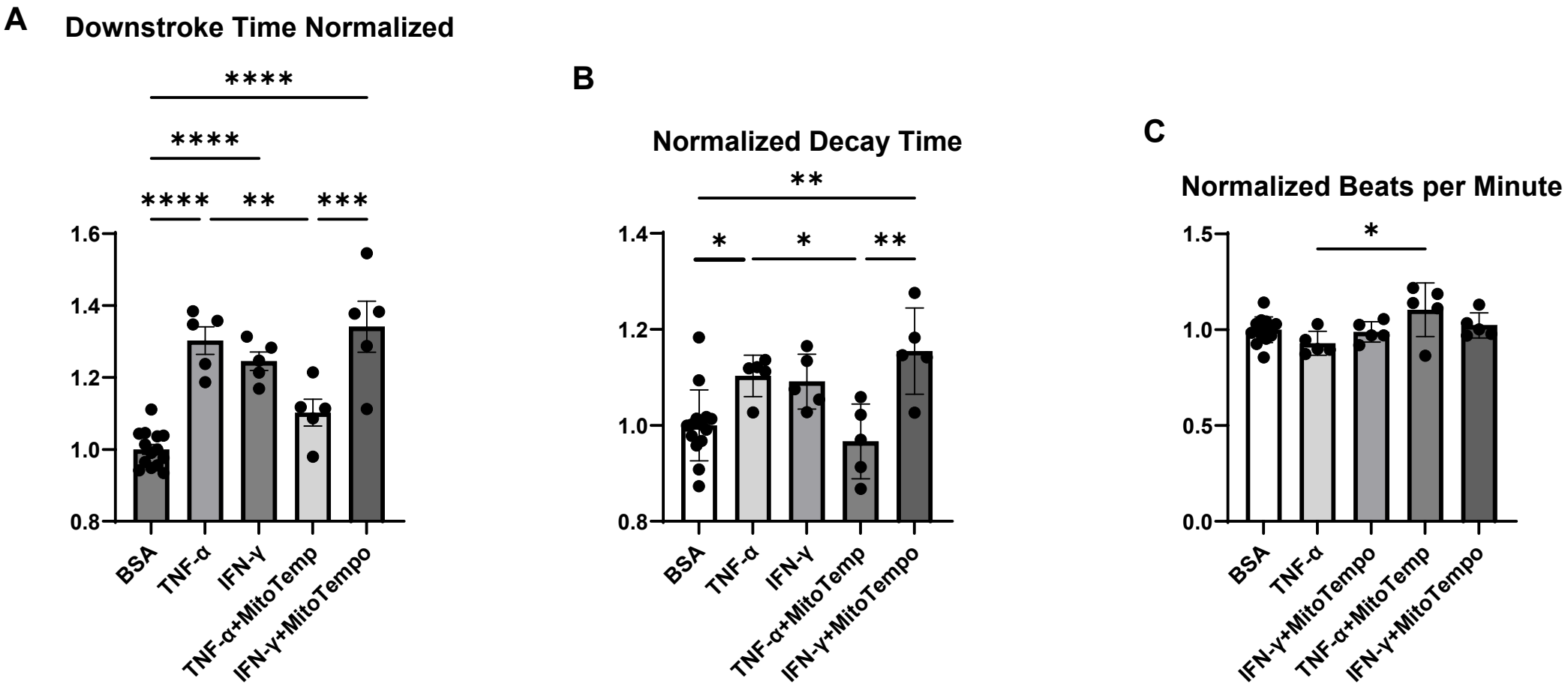
A
Downstroke Time Normalized
****
****
****
**
***
1.6
1.4
1.2
1.0
0.8
BSA
TNF-α
IFN-γ
TNF-α+MitoTemp
IFN-γ+MitoTempo
B
Normalized Decay Time
**
*
*
**
1.4
1.2
1.0
0.8
BSA
TNF-α
IFN-γ
TNF-α+MitoTemp
IFN-γ+MitoTempo
C
Normalized Beats per Minute
*
1.5
1.0
0.5
0.0
BSA
TNF-α
IFN-γ+MitoTempo
TNF-α+MitoTemp
IFN-γ+MitoTempo

Figure 2

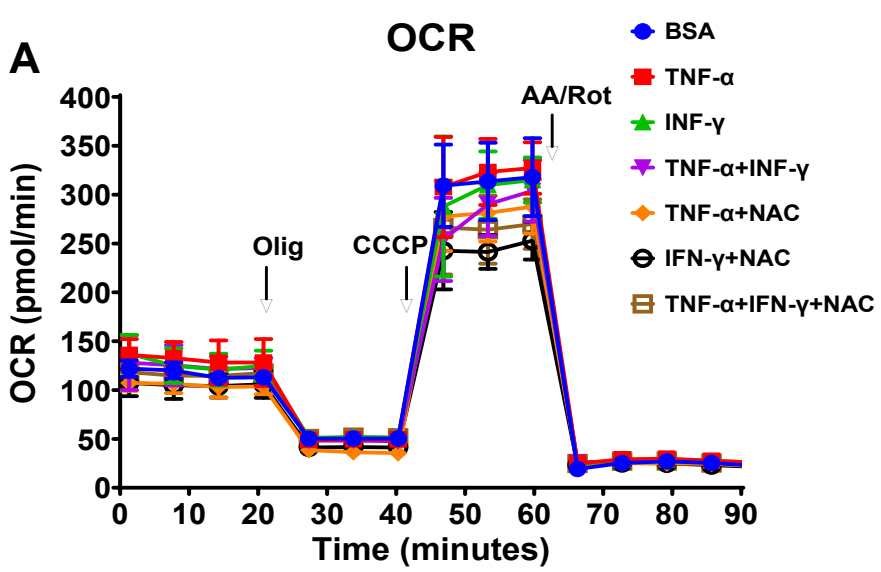
A
OCR
BSA
TNF-α
INF-γ
TNF-α+INF-γ
TNF-α+NAC
IFN-γ+NAC
TNF-α+IFN-γ+NAC
Olig
CCCP
AA/Rot
OCR (pmol/min)
Time (minutes)

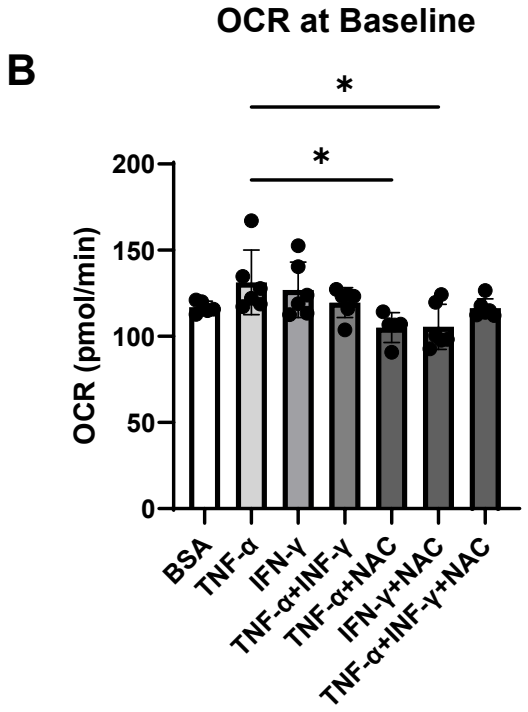
B
OCR at Baseline
*
*
OCR (pmol/min)
BSA
TNF-α
IFN-γ
TNF-α+INF-γ
TNF-α+NAC
IFN-γ+NAC
TNF-α+INF-γ+NAC

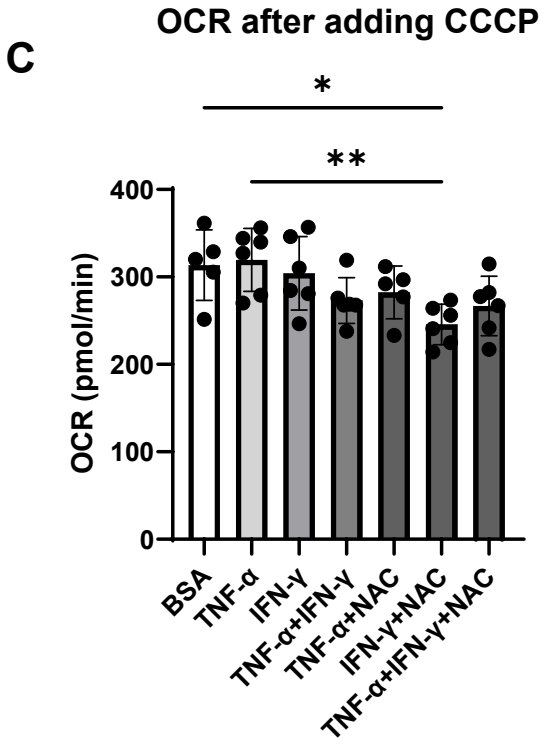
C
OCR after adding CCCP
*
**
OCR (pmol/min)
BSA
TNF-α
IFN-γ
TNF-α+IFN-γ
TNF-α+NAC
IFN-γ+NAC
TNF-α+IFN-γ+NAC

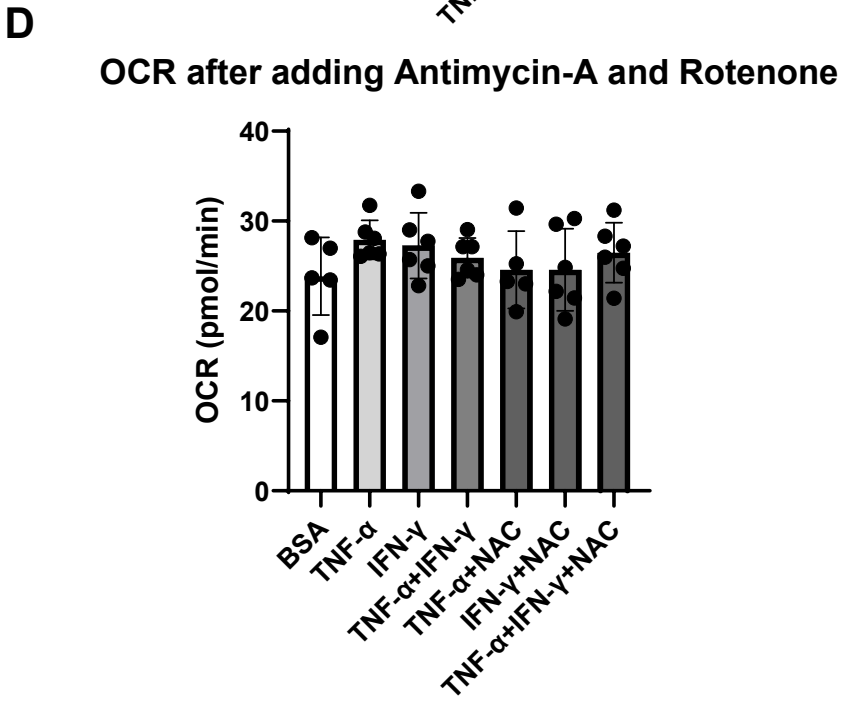
D
OCR after adding Antimycin-A and Rotenone
OCR (pmol/min)
BSA
TNF-α
IFN-γ
TNF-α+IFN-γ
TNF-α+NAC
IFN-γ+NAC
TNF-α+IFN-γ+NAC

Figure 3

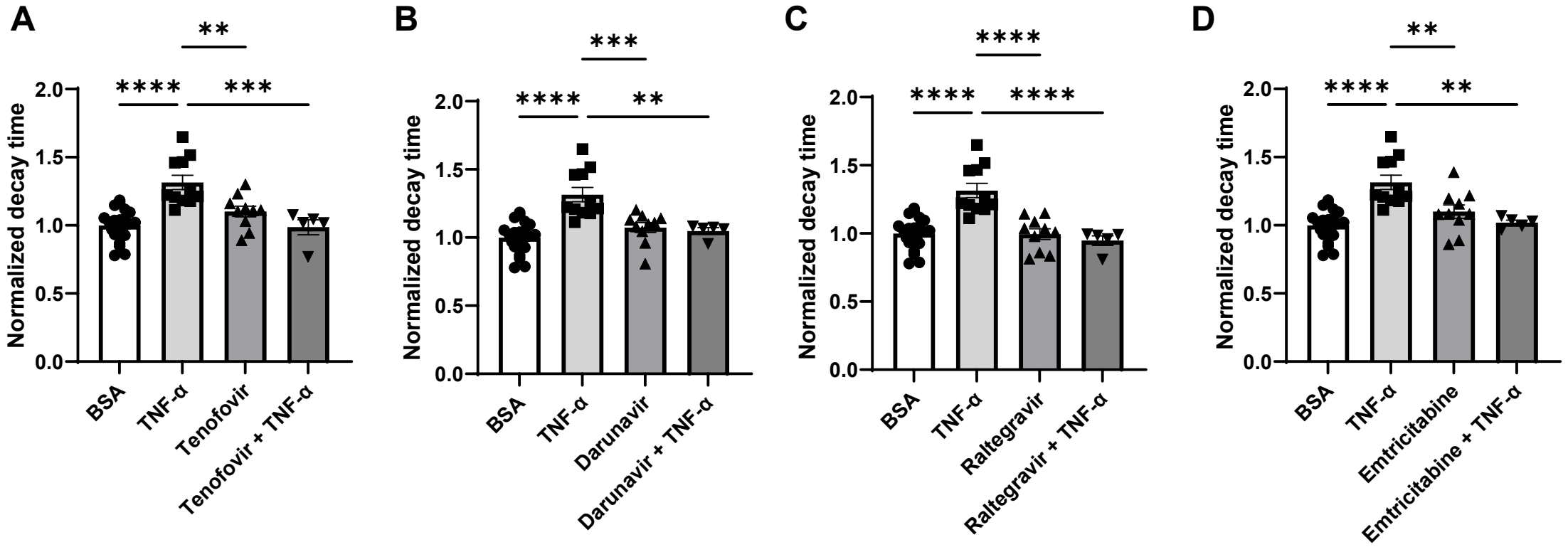
A
B
C
D
Normalized decay time
2.0
1.5
1.0
0.5
0.0
****
***
**
BSA
TNF-α
Tenofovir
Tenofovir + TNF-α
Darunavir
Darunavir + TNF-α
Raltegravir
Raltegravir + TNF-α
Emtricitabine
Emtricitabine + TNF-α

Figure 4

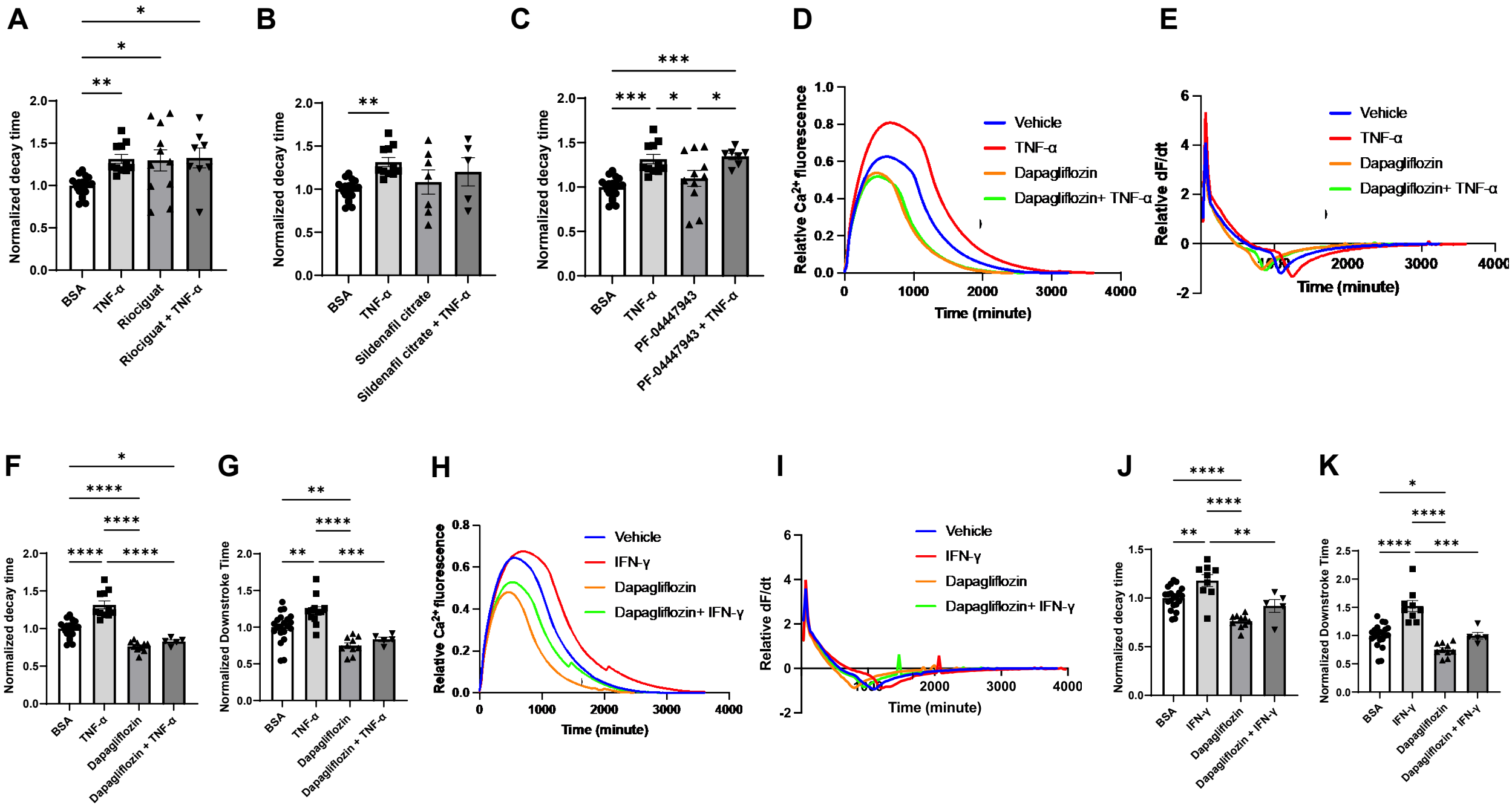
A
Normalized decay time
BSA
TNF-α
Riociguat
Riociguat + TNF-α
B
Normalized decay time
BSA
TNF-α
Sildenafil citrate
Sildenafil citrate + TNF-α
C
Normalized decay time
BSA
TNF-α
PF-04447943
PF-04447943 + TNF-α
D
Relative Ca2+ fluorescence
Time (minute)
Vehicle
TNF-α
Dapagliflozin
Dapagliflozin+ TNF-α
E
Relative dF/dt
Time (minute)
Vehicle
TNF-α
Dapagliflozin
Dapagliflozin+ TNF-α
F
Normalized decay time
BSA
TNF-α
Dapagliflozin
Dapagliflozin + TNF-α
G
Normalized Downstroke Time
BSA
TNF-α
Dapagliflozin
Dapagliflozin + TNF-α
H
Relative Ca2+ fluorescence
Time (minute)
Vehicle
IFN-γ
Dapagliflozin
Dapagliflozin+ IFN-γ
I
Relative dF/dt
Time (minute)
Vehicle
IFN-γ
Dapagliflozin
Dapagliflozin+ IFN-γ
J
Normalized decay time
BSA
IFN-γ
Dapagliflozin
Dapagliflozin + IFN-γ
K
Normalized Downstroke Time
BSA
IFN-γ
Dapagliflozin
Dapagliflozin + IFN-γ

Figure 5

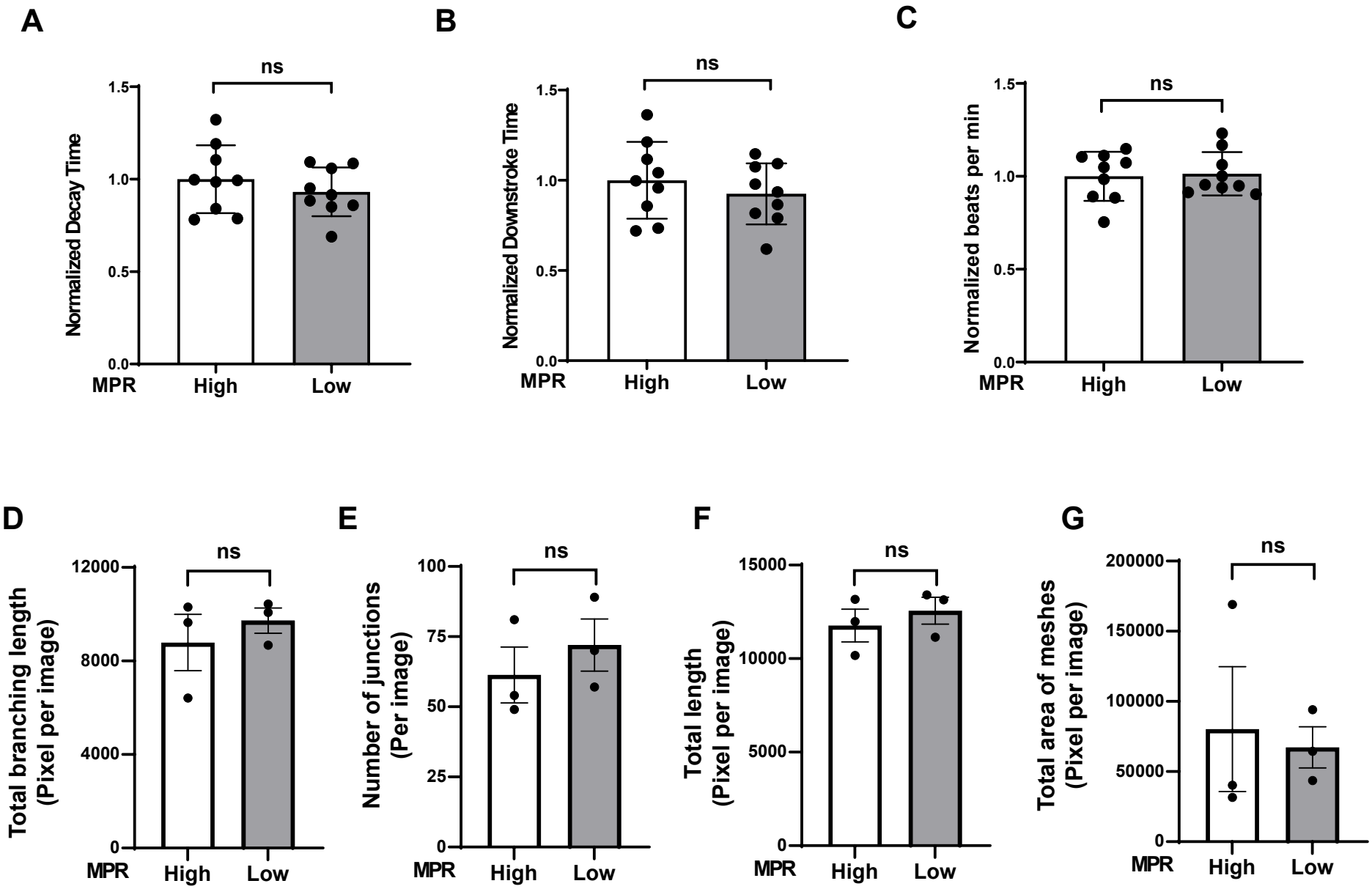
A
ns
Normalized Decay Time
1.5
1.0
0.5
0.0
MPR
High
Low
B
ns
Normalized Downstroke Time
1.5
1.0
0.5
0.0
MPR
High
Low
C
ns
Normalized beats per min
1.5
1.0
0.5
0.0
MPR
High
Low
D
ns
Total branching length
(Pixel per image)
12000
8000
4000
0
MPR
High
Low
E
ns
Number of junctions
(Per image)
100
75
50
25
0
MPR
High
Low
F
ns
Total length
(Pixel per image)
15000
10000
5000
0
MPR
High
Low
G
ns
Total area of meshes
(Pixel per image)
200000
150000
100000
50000
0
MPR
High
Low

Figure 6

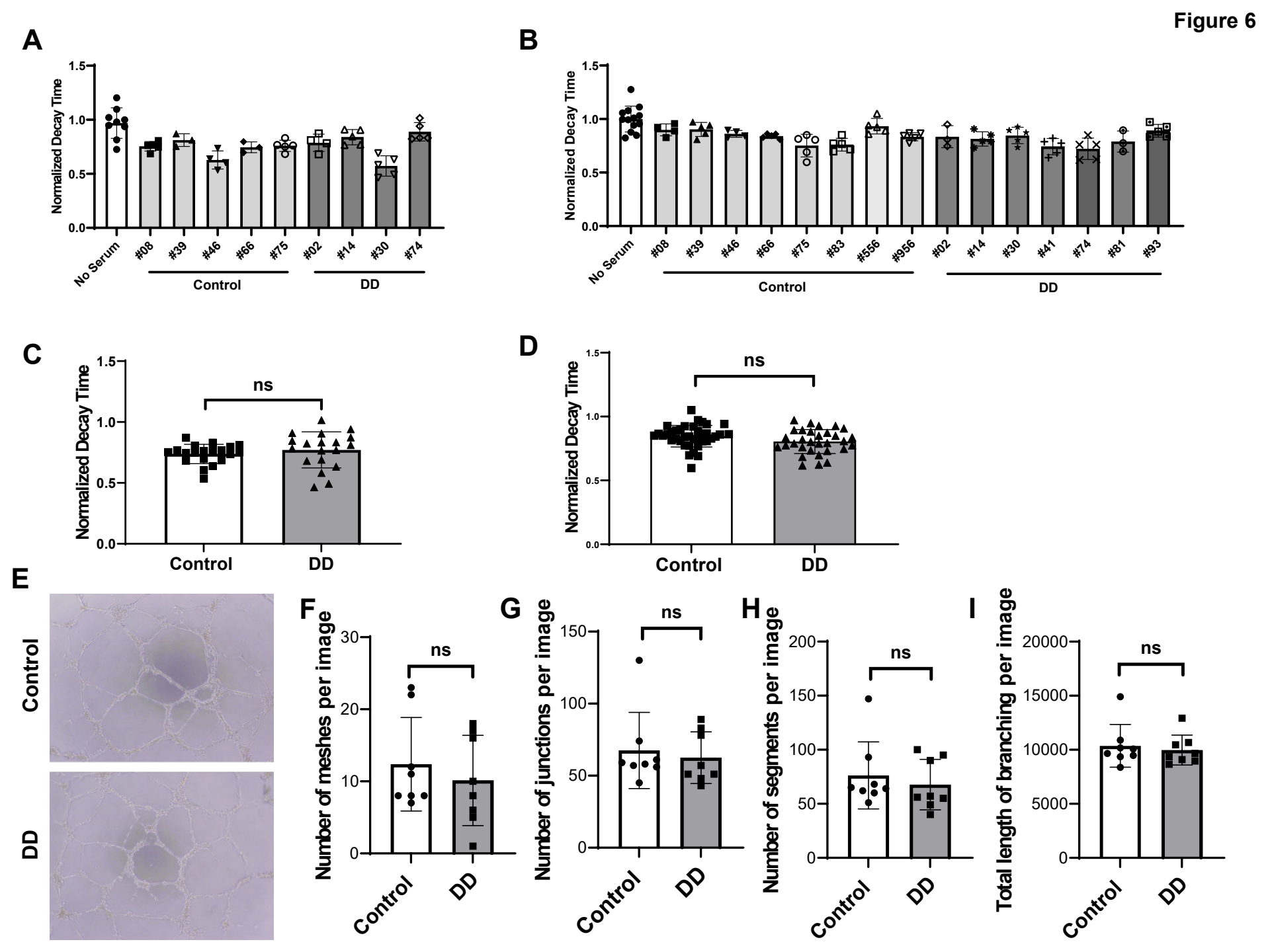
A
Normalized Decay Time
1.5
1.0
0.5
0.0
No Serum
#08
#39
#46
#66
#75
#02
#14
#30
#74
Control
DD
B
Normalized Decay Time
No Serum
#08
#39
#46
#66
#75
#83
#556
#956
#02
#14
#30
#41
#74
#81
#93
Control
DD
C
Normalized Decay Time
ns
Control
DD
D
Normalized Decay Time
ns
Control
DD
E
Control
DD
F
Number of meshes per image
ns
30
20
10
0
Control
DD
G
Number of junctions per image
ns
150
100
50
0
Control
DD
H
Number of segments per image
ns
200
150
100
50
0
Control
DD
I
Total length of branching per image
ns
20000
15000
10000
5000
0
Control
DD

Figure 1-figure supplement 1

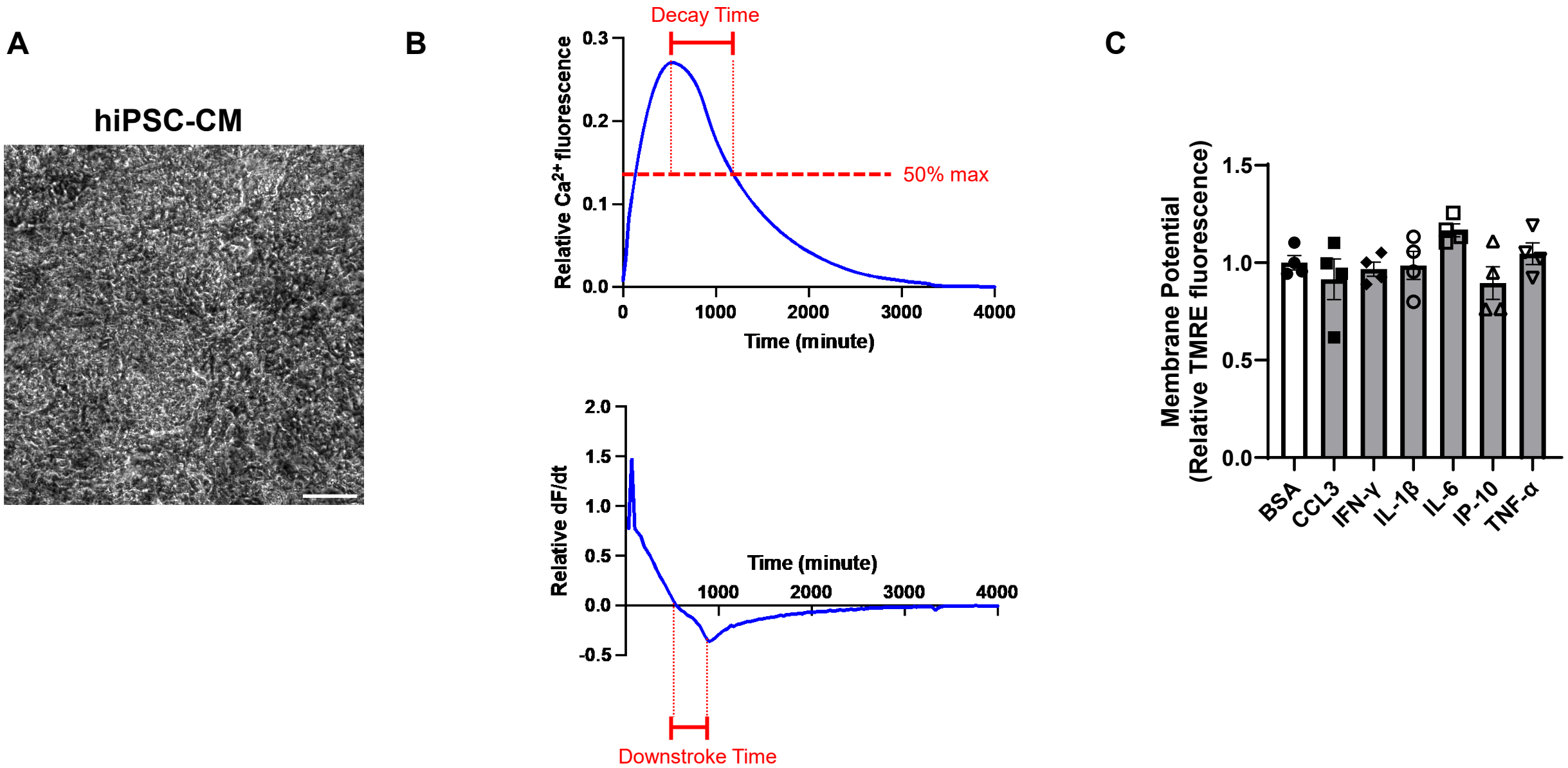

Figure 3-figure supplement 1

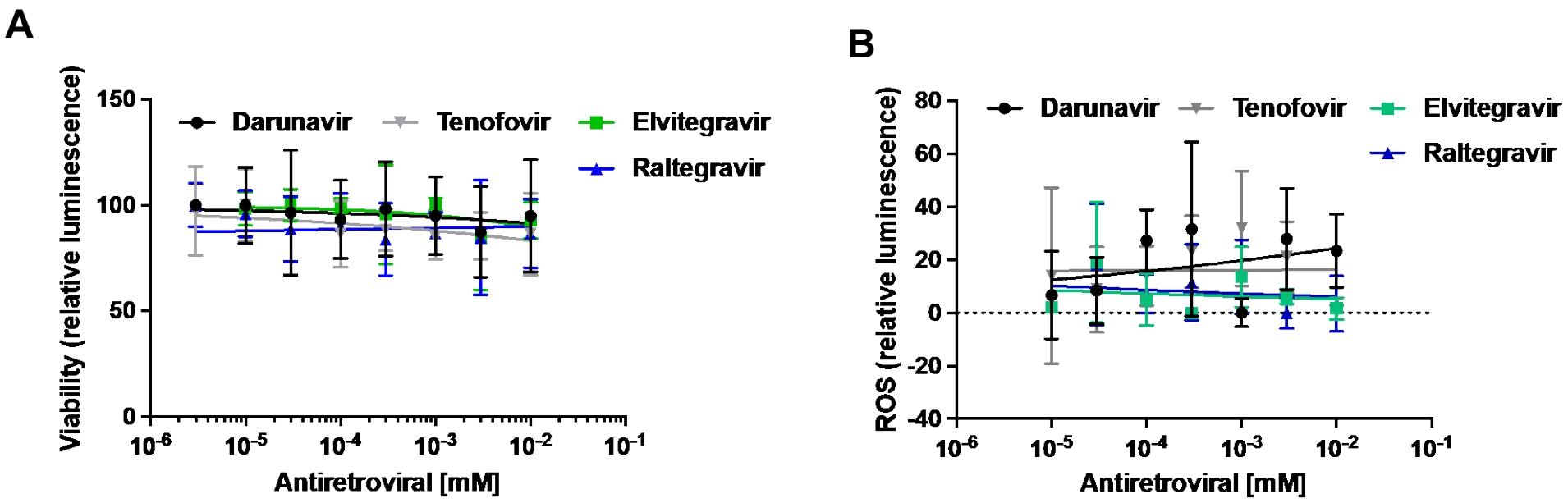

Figure 4-figure supplement 1

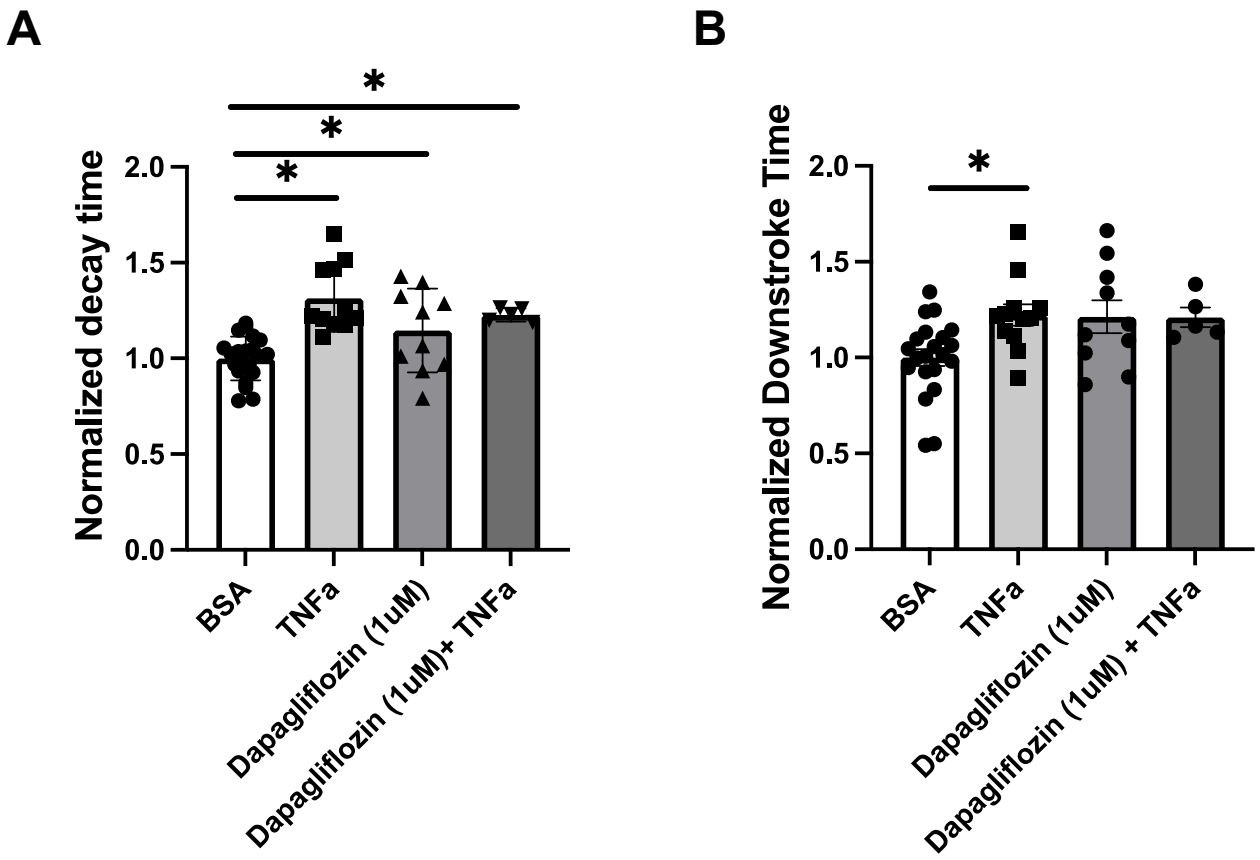

Figure 5-figure supplement 1

20h **2% serum**

4x

High MPR (Control)

Low MPR (DD)

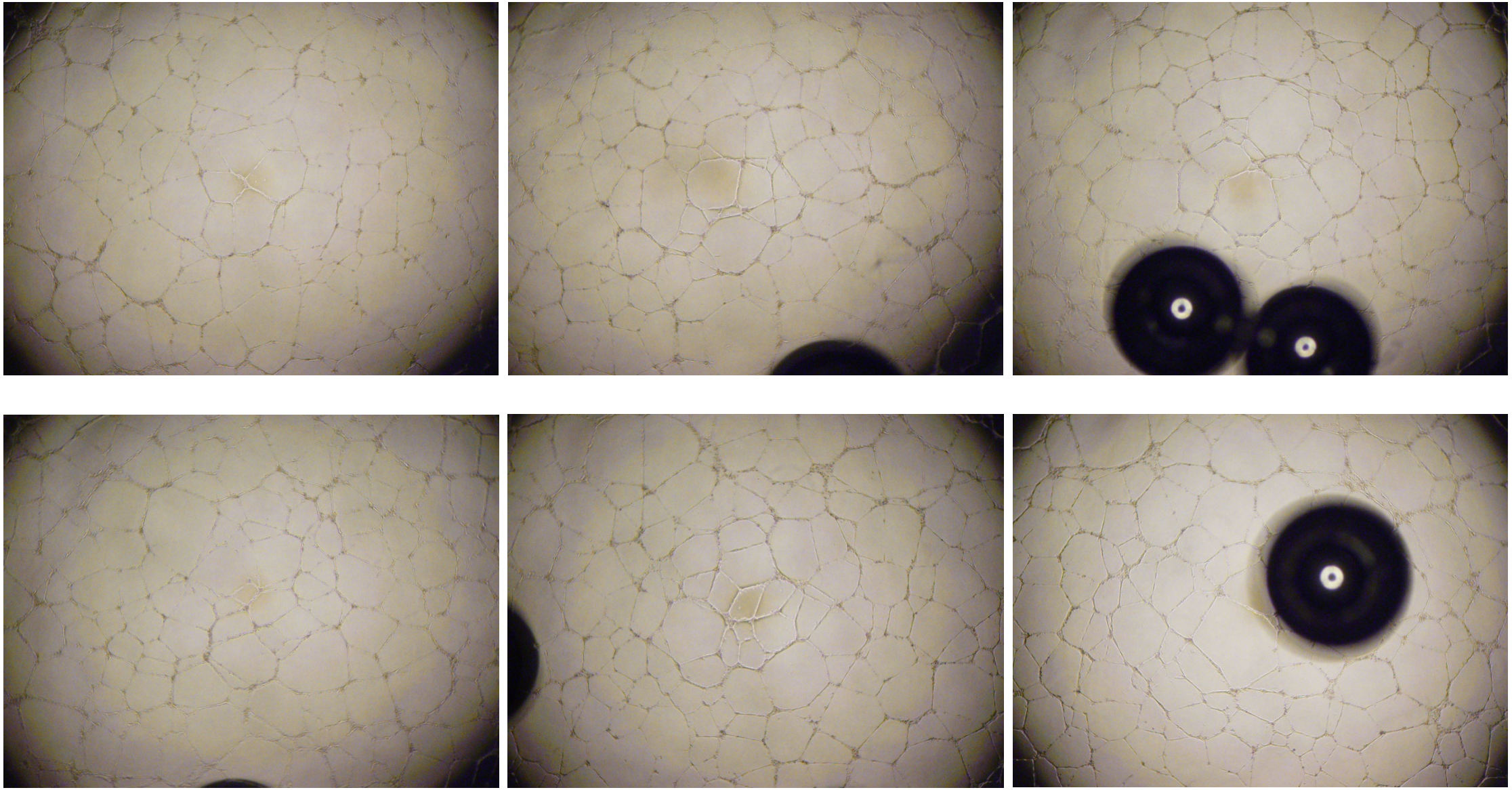

Figure 5-figure supplement 2

20h **2% serum**

10x

High MPR (Control)

Low MPR (HFpEF)

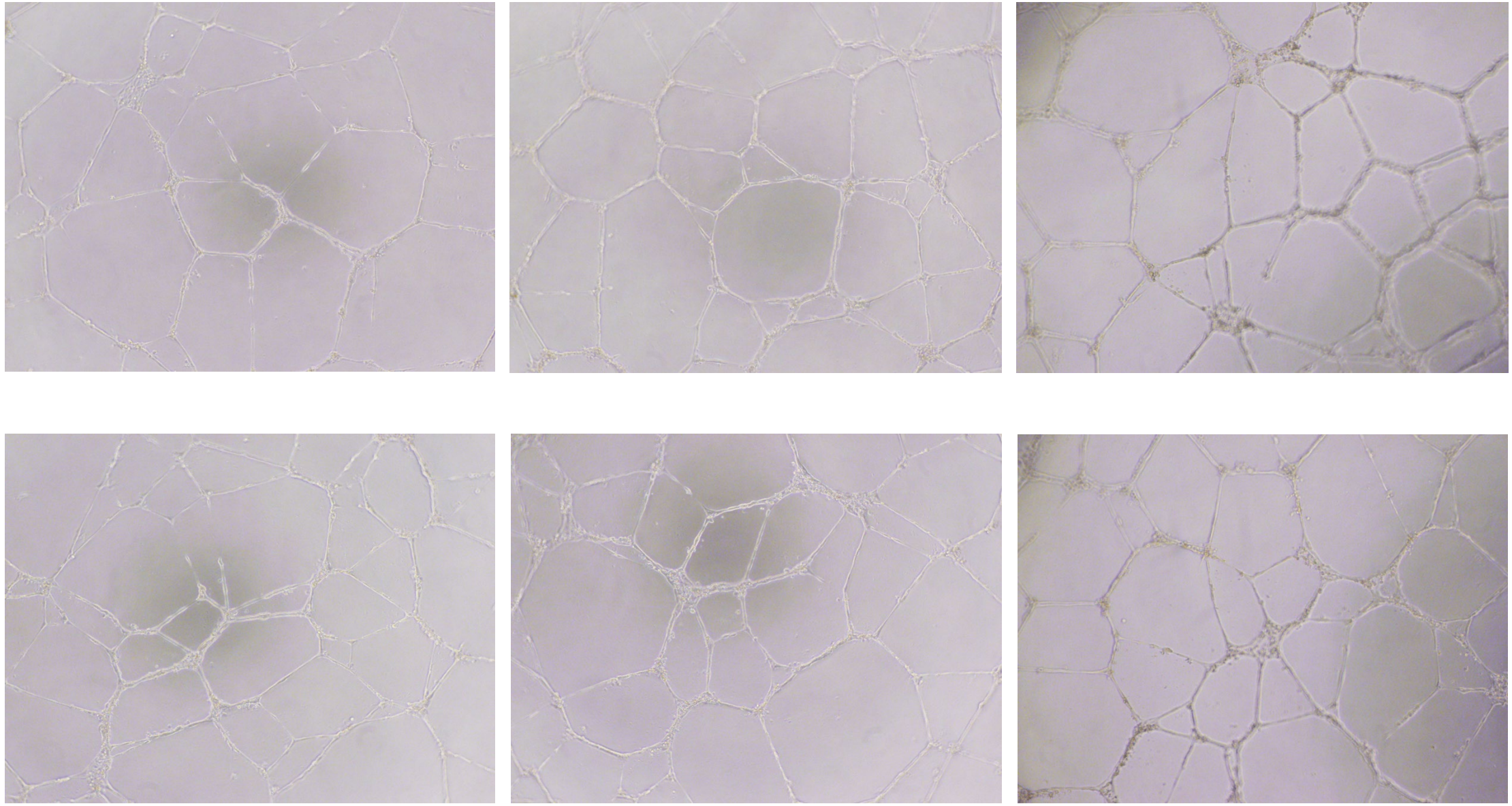

Supplementary Table 1. Clinical characteristics of study population for Group 1

Participant	Age	High or low MPR group	Sex	CD4 count	Diabetes Mellitus?	Active cigarette smoking?	Hypertension?	Coronary artery disease diagnosis?	Left ventricular ejection fraction (LVEF)	Myocardial perfusion reserve (MPR)
1	50	High	Male	487	No	Yes	Yes	No	64	2.74
2	62	Low	Male	703	No	No	Yes	Yes	59	1.03
3	64	High	Male	321	No	No	No	Yes	65	3.43
4	55	High	Male	749	No	No	Yes	Yes	59	1.90
5	71	Low	Male	1743	No	No	Yes	Yes	55	1.03
6	59	Low	Male	678	No	No	Yes	No	52	1.13